Table II
Ratio of Diffusion Constants for Linear and Cyclic Chains

N	D_{cm}(linear)/D_{cm}(cyclic)	N	D_{cm}(linear)/D_{cm}(cyclic)
16	5.40	128	3.22
32	3.83	256	2.44
64	3.37		

chain length as also can be seen from dependencies shown in Figure 11. Unfortunately, it is not possible from the present data to estimate the asymptotic behavior of cyclic chains at $N \rightarrow \infty$. We expect a small constant value of the ratio D_{cm}(linear)/D_{cm}(cyclic) at this limit. Considering that the diffusion constants for the linear chains are decreasing with chain length faster at the longest chain lengths considered than those for the ring chains, the possibility that the linear chains can become slightly slower than their cyclic analogues at the limit $N \rightarrow \infty$ cannot be excluded. In any case, the results presented here indicate that the mechanism of motion based on cooperative rearrangements within closed loops leads to comparable mobilities of linear and cyclic chains with the ratio of diffusion constants decreasing with increasing chain length. The larger difference in diffusion constants for short chains can be attributed to large concentrations of chain ends in systems with linear chains, which change considerably the density of position-exchange possibilities. Calculations for systems with longer chains are certainly necessary. This would demand, however, calculation times that are not available to us at the moment.

Conclusions

Results presented in this article demonstrate that application of the mechanism of cooperative motions within closed loops to ordered systems with cyclic chains filling the space completely involves a kind of "melting" process leading to equilibrated states in which cyclic chains are randomly coiled but slightly collapsed in comparison to Gaussian chains. The last effect is attributed to topological constraints imposed on cyclic chains by noncrossability and close packing.

The translational diffusion of cyclic chains in such systems is also demonstrated. The analysis of monomer displacements shows that the behavior of cyclic chains is qualitaively the same as that observed previously for systems with linear chains. The diffusion constant of the center of mass of short cyclic chains is found to be remarkably smaller than that for linear chains of equivalent length. With increasing chain length, however, the ratio of diffusion constants decreases, so that the rates of self-diffusion of linear and cyclic chains can be regarded as comparable.

References and Notes

(1) Zimm, B. H.; Stockmayer, W. H. *J. Chem. Phys.* **1949**, *17*, 1301.
(2) Casassa, E. F. *J. Polym. Sci., Part A* **1965**, *3*, 605.
(3) Fukatsu, M.; Kurata, M. *J. Chem. Phys.* **1966**, *44*, 4539.
(4) Bloomfield, V.; Zimm, B. H. *J. Chem. Phys.* **1966**, *44*, 315.
(5) Kumbar, M. J. *J. Chem. Phys.* **1973**, *59*, 5620.
(6) Martin, J. E.; Eichinger, B. E. *Macromolecules* **1983**, *16*, 1345.
(7) Dodgson, K.; Semlyen, J. A. *Polymer* **1978**, *19*, 1285.
(8) Clarson, S. J.; Dodgson, K.; Semlyen, J. A. *Polymer* **1985**, *26*, 980.
(9) Hild, G.; Strazielle, C.; Rempp, P. *Eur. Polym. J.* **1983**, *19*, 721.
(10) Geiser, D.; Hocher, H. *Macromolecules* **1980**, *13*, 653.
(11) Roovers, J.; Toporowski, P. M. *Macromolecules* **1983**, *16*, 843.
(12) Hadziioannou, G.; Cotts, P. M.; ten Brinke, G.; Han, C. C.; Lutz, P.; Strazielle, C.; Rempp, P.; Kovacs, A. J. *Macromolecules* **1987**, *20*, 493.
(13) Semlyen, J. A. *Pure Appl. Chem.* **1981**, *53*, 1797.
(14) Dodgson, K.; Baunister, O. J.; Semlyen, J. A. *Polymer* **1980**, *21*, 663.
(15) McKenna, G. B.; Hadziioannou, G.; Lutz, P.; Hild, G.; Strazielle, C.; Straupe, C.; Rempp, P.; Kovacs, A. J. *Macromolecules* **1987**, *20*, 498.
(16) Roovers, J. *Macromolecules* **1985**, *18*, 1359.
(17) Klein, J. *Polym. Prepr. (Am. Chem. Soc., Div. Polym. Chem.)* **1981**, *22*, 105.
(18) Klein, J. *Macromolecules* **1986**, *19*, 105.
(19) de Gennes, P.-G. *J. Chem. Phys.* **1971**, *45*, 572.
(20) Doi, M.; Edwards, S. F. *J. Chem. Soc., Faraday Trans. 2* **1987**, *74*, 1789, 1802, 1818.
(21) Klein, J. *Macromolecules* **1978**, *11*, 852.
(22) Pakula, T. *Macromolecules* **1987**, *20*, 679.
(23) Pakula, T.; Geyler, S. *Macromolecules* **1987**, *20*, 2909.
(24) Yoon, D. Y.; Baumgartner, A. *Macromolecules* **1983**, *17*, 2864.
(25) Pakula, T. *Polymer* **1987**, *28*, 1293.
(26) Yamakawa, H. *Modern Theory of Polymer Solutions*; Harper and Row: New York, 1971.
(27) des Cloizeaux, J.; Mehta, M. L. *J. Phys. (Les Ulis, Fr.)* **1979**, *40*, 665.
(28) Mills, P. J.; Mayer, J. W.; Kramer, E. J.; Hadziioannou, G.; Lutz, P.; Strazielle, C.; Rempp, P.; Kovacs, A. J. *Macromolecules* **1987**, *20*, 513.
(29) Cates, M. E.; Deutsch, J. M. *J. Phys. (Les Ulis, Fr.)* **1986**, *47*, 2121.

Theory of Thermoelastic Properties for Polymer Glasses

Elisabeth Papazoglou and Robert Simha*

Department of Macromolecular Science, Case Western Reserve University, Cleveland, Ohio 44106.

Received September 14, 1987; Revised Manuscript Received November 12, 1987

ABSTRACT: We derive expressions for the extensional elastic moduli as functions of temperature and pressure by a generalization of the equation of state theory. Our previous efforts in this direction were confined to the low-temperature region, where the characteristic free volume function, defined by theory, is effectively frozen. We proceed now to higher temperatures, where the temperature and pressure dependence of this function play a decisive role. The static Young's and shear modulus and the Poisson ratio are computed, based solely on equation of state information. This is illustrated by means of applications to poly(vinyl acetate) glasses at low and elevated pressures and for different formation histories. Further comparisons with experimental results are presented for poly(methyl methacrylate). A unified treatment of static compressional and elongational properties thus exists, at present for the linear regime of deformations. We conclude with an outline of possible extensions.

1. Introduction

In recent years the configurational thermodynamic or quasi-thermodynamic properties of amorphous polymers in the melt and glassy states have been receiving intensive experimental and theoretical attention. Quantitatively successful formulations for single and multiconstituent systems were obtained. They are based on a lattice model which incorporates a particular structure function and

0024-9297/88/2221-1670$01.50/0

introduces additional disorder in the form of a vacancy or excess free volume fraction. This function was shown to play an important role in subsequent extensions of the theory to the kinetics of physical aging processes in polymer glasses.

In a second extension we have started an investigation of thermoelastic properties in the glassy state by introducing anisotropic stresses in the model referred to above.[1,2] It has been shown previously[3] that the thermal expansivity of polymer glasses between about 10 to 50 K could be predicted by assuming that the free volume fraction was practically frozen. We note in passing that this can also satisfactorily account for the PVT properties of crystalline polymers.[4] These findings have now been extended to obtain a *second* elastic constant, i.e., Young's or shear modulus, and Poisson ratio at extremely low temperatures, once the equation of state and hence the bulk modulus are known. A combination of experiment and theory shows that at higher temperatures, the free volume exhibits a significant temperature and pressure dependence.[5]

The purpose of this paper is to develop a theory of the temperature- and pressure-dependent elastic constants in the temperature range between about T_β and T_g, based on information about the equation of state. In section 2 prerequisite matters are restated and the new results of the theory are derived. Section 3 contains applications to glasses of varying formation histories. A short account of this work has appeared.[6]

2. Theory

A. The Undeformed System. As indicated in section 1, a knowledge of the bulk modulus $K = -V(\partial p/\partial V)_T$ is a prerequisite. We shall at the outset remain in the linear elastic range and thus this derivative is to be taken at zero strain, as derived from the pressure equation

$$p = -(\partial F/\partial V)_T \tag{1}$$

with F the Helmholtz free energy. The essence of the model to be employed is depicted on the upper half of Figure 1. It shows one of the cells spanning the system, with a central chain segment surrounded by other segments located on the sites of a (quasi) lattice and by unoccupied sites. Let $y(V,T)$ denote the temperature- and volume-dependent fraction of occupied sites. Then eq 1 becomes

$$-p = (\partial F/\partial V)_{T,y} + (\partial F/\partial y)_{T,V}(\partial y/\partial V)_T \tag{2}$$

From the model the first two derivatives are derived as functions of V, T, and y. As is elaborated in ref 5 (1976), these expressions are combined with the results of PVT measurements, to obtain by means of eq 2 $y(V,T)$ for, of course, a specified formation history (cooling rate, formation pressure) of the glass. This information is then utilized as a point of departure for the computation of y_d, the corresponding function in the deformed body. Ultimately, as is to be shown, this yields ΔF, the free energy change as a function of strain ϵ. In the linear elastic range, ΔF is to be computed up to $\mathcal{O}(\epsilon^2)$.

The free energy derivatives appearing in eq 2 are given by the following expresions:[5]

$$(\partial \tilde{F}/\partial \tilde{V})_{\tilde{T},y} = -(\tilde{T}/\tilde{V})[1 - 2^{-1/6}y\tilde{\omega}^{-1/3}]^{-1} - (2y/\tilde{V})\tilde{\omega}^{-2}[1.011\tilde{\omega}^{-2} - 1.2045]$$

$$(\partial \tilde{F}/\partial y)_{\tilde{T},\tilde{V}} = -(3\tilde{T}/y) \times (s/3c)[(s-1)/s + \ln(1-y)/y] + (3\tilde{T}/y)[2^{-1/6}y\tilde{\omega}^{-1/3} - 1/3][1 - 2^{-1/6}y\tilde{\omega}^{-1/3}]^{-1} + 0.5\tilde{\omega}^{-2}(2.409 - 3.033\tilde{\omega}^{-2}) \tag{3}$$

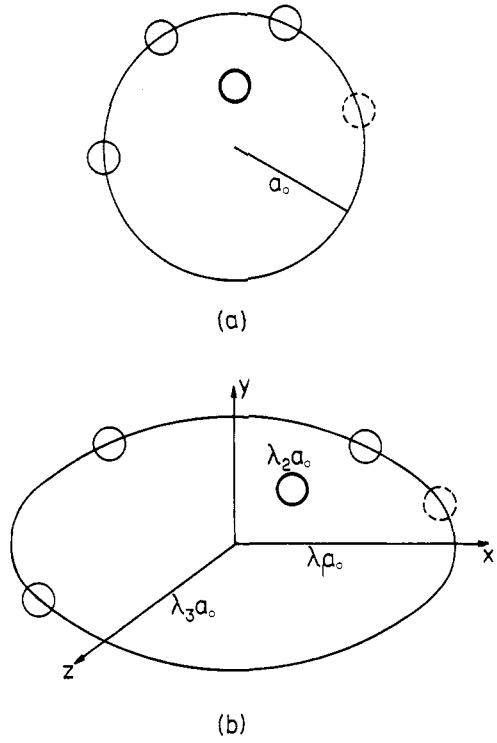

Figure 1. (a) Original cell: heavy line, reference segment; dashed line, vacancy. (b) Cell under uniaxial strain: λ_1; $\lambda_2 = \lambda_3$.

Equations 1–3 then yield the compression modulus with $3c/s$, the number of external degrees of freedom per segment, set equal to unity and $s \to \infty$.

$$\tilde{K} = -\tilde{V}(\partial \tilde{p}/\partial \tilde{V})_T = -\tilde{V}(\partial \tilde{p}/\partial \tilde{V})_{T,y} - \tilde{V}(\partial \tilde{p}/\partial y)_{T,V}(\partial y/\partial \tilde{V})_T$$

$$\tilde{K} = (\tilde{T}/\tilde{V})/A1 - (2^{-1/6}/3)\tilde{\omega}^{-2/3}/(A1)^2 + (2y\tilde{\omega}^{-2}/\tilde{V}) \times (5.055\tilde{\omega}^{-2} - 3.6135) - (\partial y/\partial \tilde{V})_T[12.132\tilde{\omega}^{-4} - 4.818\tilde{\omega}^{-2} - (\tilde{T}\tilde{V}/y)(A1 + A2)(1 - A1)/(A1)^2 - \tilde{T}(A3)/(A1)^2] - (\partial y/\partial \tilde{V})_T^2\tilde{T}\tilde{V}[\ln(1-y)/y^3 + y^{-3} - y^{-2}/(1-y) - (3/y^2)(A2/A1) - (3/y)(A3)(A1 + A2)/(A1)^2 + 6.0664\tilde{\omega}^{-4}y^{-1}/\tilde{T} - 2.409\tilde{\omega}^{-2}y^{-1}\tilde{T}] \tag{4}$$

with

$$A1 = 1 - 2^{-1/6}y\tilde{\omega}^{-1/3}$$

$$A2 = 2^{-1/6}y\tilde{\omega}^{-1/3} - 1/3 \qquad A3 = (2/3)2^{-1/6}y^{-4/3}\tilde{\omega}^{-1/3}$$

Here the tildes indicate quantities scaled in terms of characteristic variables of state p^*, V^*, and T^*, derived from the equation of state of the melt and retained in the glass, and $\omega = yV$.

In ref 5 (1976), eq 2 is solved for two glasses of poly(vinyl acetate) (PVAc), which have been formed by cooling at a fixed rate under atmospheric pressure and 80 MPa (referred to in section 3 as low- and high-pressure glass). The solutions are conveniently given as polynomials in V and T and p and T. Alternatively, the complications and efforts involved in this solution procedure are bypassed when only the first derivative in eq 2 is considered and y is derived as the numerical solution of an algebraic equation. The results of the two methods, designated as partition function (PF) and adjusting parameter (AP) methods[5] have been compared in detail. PF has been carried out only for the two PVAc glasses. For other glasses, such as poly(methyl methacrylate) (PMMA) and polystyrene (PS) only AP results are available.[7] The numerical differences between the computed free volume fractions are small, as may be judged by an inspection of Figure 10 in ref 5 (1976).

Before proceeding, we recall that the empirical Tait equation has been frequently employed both for the melt and glass, to represent experimental PVT data and to facilitate the comparison between experiment and prediction. The expression for the bulk modulus in terms of the quantities, C, a constant, and B, a temperature function, then becomes

$$C \times K(\text{Tait}) = (B + p)V(T, p)/V(T,0)$$

with

$$V(T,p)/V(T,0) = 1 - C \ln (1 + p/B) \quad (5)$$

$$B(T) = B_0 \exp(-B_1 T)$$

Differences between eq 4 and 5 will arise, even when the computed volumes are close, and it does not necessarily follow that the latter is more accurate than the former.

B. Deformational Free Energy. Our previous investigations[1,2] were based on the assumption of affine deformation. That is, the macrocopic, imposed strain pattern is to be *identically* reproduced on the microscopic scale. In the context of the present model, this implies uniformity from cell to cell. One might think of allowing for fluctuations, i.e., for negative and positive departures in different cells, adding up to the imposed magnitudes of strain. This introduces correlations between happenings in different cells. In its simplest version, however, cell theory does not allow for interactions between the central units in different cells and presumes happenings in one cell to be identically reproduced in all others.

The particular choice of the strain patterns to be applied and hence the second modulus to be obtained are at our disposal. As previously[1,2] we find it convenient in what follows to consider a uniaxial elongation[1,2] (ϵ_1) and derive expressions for Young's modulus Y by means of the relation[8]

$$Y = \lim_{\epsilon \to 0} (1/V)(\partial^2 F/\partial \epsilon^2)_T - p \quad (6)$$

The free energy F in the undeformed state contains three contributions,[9] namely, a free volume term, V_f, a lattice energy, E, and a combinatory factor, referring to the mixing of occupied and empty sites in the lattice. All of these involve the y-function which now changes for a given V and T from $y(V,T)$ to $y_d(V,T,\epsilon)$, where ϵ symbolizes a particular strain pattern. The spherical symmetry of the original cell is now converted into the symmetry of an ellipsoid of revolution;[1,2] see Figure 1. Its axes are $\lambda_i a_0$, where for the uniaxial elongation $\lambda_1 = 1 + \epsilon_1$ and $\lambda_2 = \lambda_3 = 1 - \epsilon_2 = 1 - \mu\epsilon_1$, with μ the Poisson constant and a_0 the radius of the spherical cell. The configurational free energy for the deformed system F_d can then be written as

$$F_d(V,T,y_d;\epsilon) = (N/2)y_d E(\epsilon \neq 0) - NkT \ln V_{f,d} + NkT \ln y_d - NkT(1 - 1/y_d) \ln (1 - y_d) \quad (7)$$

Consider now each term, starting with the lattice energy E. It has already been computed,[1] being the sole contribution at $T = 0$. The result is

$$\tilde{E} = 1.011\tilde{\omega}^{-4} - 2.049\tilde{\omega}^{-2} + 4(\epsilon_1 - 2\epsilon_2) \times (1.2045\tilde{\omega}^{-2} - 1.011\tilde{\omega}^{-4}) + \epsilon_1^2(16.04\tilde{\omega}^{-4} - 10.4386\tilde{\omega}^{-2}) + \epsilon_2^2(42.326\tilde{\omega}^{-4} - 27.302\tilde{\omega}^{-2}) - \epsilon_1\epsilon_2(20.4866\tilde{\omega}^{-4} - 12.848\tilde{\omega}^{-2}) \quad (8)$$

Here $\tilde{\omega} = y\tilde{V}$ represents the reduced cell volume and the numerics include second and third shell interactions.

In the formulation of the free volume term V_{fd}, we continue with the adoption of a linear averaging of properly weighted "solid" and "gas"-like modes.[9] Hence we have

$$\tilde{V}_{fd} = [y_d \tilde{V}_{f,ds}^{1/3} + (1 - y_d)\tilde{\omega}^{1/3}(1 + \epsilon_1 - 2\epsilon_2)^{1/3}]^3 \quad (9)$$

The second term relates to the cell volume and takes into account the change in volume resulting from strains ϵ_1 and ϵ_2. The first term represents the accessible volume within one cell in the absence of holes. For $\epsilon = 0$, this is a sphere of radius $a_0 - \sigma$, with σ the repulsion radius of the units, smeared out over the cell surface and surrounding the central unit.[10] The corresponding expression for the deformed cell, eq A-6, is derived in the Appendix.

The final issue is the relation between y and y_d. We recall that y was extracted by a combination of F derivatives with PVT data. One might contemplate an analogous approach by introducing at this point stress–strain measurements. Our aim, however, is the prediction of elastic properties, based *exclusively* on properly evaluated equation of state information. Various a priori working hypotheses may be considered. As is illustrated by our previous work,[2] the theory of linear elasticity serves as an important guide and imposes restrictions in this matter. These arise from the following equation of linear elasticity:

$$Y = 3K(1 - 2\mu) \quad (10)$$

On the other hand, eq 6 and 7 involve a relation between Y and μ for a given K. Incorrect assumptions for y_d will be reflected in unphysical values and variations of the computed elastic constants. It is of interest to illustrate some of these assumptions.

The simplest proposition is to determine the change in the free volume fraction arising solely from the change in cell volume upon deformation. Then one has

$$y_d = y[1 - \epsilon_1 + 2\epsilon_2 + (\epsilon_1 - 2\epsilon_2)^2] \quad (11)$$

disregarding higher powers in ϵ. The substitution in the free energy function and application to PVAc with the information about the undeformed state at hand (see section 3) yield physically unacceptable solutions.

More generally, we assume a quadratic form, viz.,

$$y_d = y(1 + g_1\epsilon_1 + g_2\epsilon_2^2) \quad (12)$$

and seek to determine the coefficients by two alternative postulates. First consider that the deformational free energy is a minimum with respect to the hole fraction y_d under strain, i.e.

$$(\partial \Delta F/\partial y_d)_{V,T,\epsilon} = 0 \quad (12a)$$

Next assume that the departure from equilibrium, as measured by the free volume derivative of the free energy, is identical in the unstrained and the strained states. Thus

$$(\partial F_d/\partial y_d)_{V,T,\epsilon} = (\partial F/\partial y)_{V,T} \quad (12b)$$

None of the above assumptions enable us to arrive at values of g_1 and g_2, yielding a reasonable Poisson constant, when evaluated again for our test case, namely, PVAc.

Dr. J. G. Curro raised the question whether the strain dependence of y_d can be deduced from the corresponding dependence of the volume (rather than the free volume fraction, eq 11), as defined by the Poisson ratio. Employing, as previously, an iteration procedure, one finds no proper, strain-independent solution for μ and Y. Thus we observe a nonequivalence of volume (or free volume) changes resulting from variations of temperature or pressure and from anisotropic stresses.

The following iteration method then, as described in the flow diagram, Figure 2, is successful. At a specified p, T, and hence K, start with a trial value of μ and compute y_d for a series of ϵ_1 values from the deformational free energy, eq 6–9, as indicated by the second step in the flow chart. In the third step, the results are fitted to a polynomial.

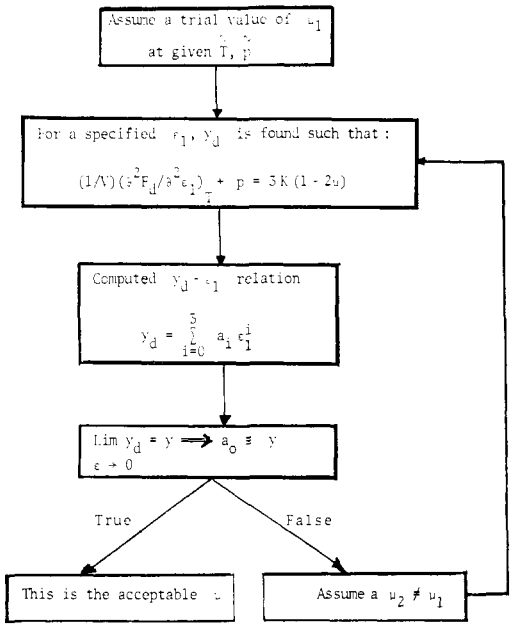

Figure 2. Flow diagram of iteration procedure. For explanation see text.

The acceptable solution for μ satisfies the stated condition on a_0. The results obtained in this manner will be seen in section 3. To recapitulate, the independence of K and the assumed μ results in a Y consistent with linear elasticity. Only y_d is a function of deformation, given by the polynomial in Figure 2, with coefficients a_i independent of ϵ.

3. Application

A. Poly(vinyl acetate). This polymer is particularly suitable for our purposes, since the equation of state, determined under two different formation conditions, has been analyzed in detail in our theoretical frame.[5] The following information about the scaling parameters and the free volume fraction $h = 1 - y$ is to be utilized:[5]

$V^* = 0.8141$ cm^3/g; $T^* = 9419$ K; $p^* = 938$ MPa

low-pressure glass, PF,

$$h(\tilde{p},\tilde{T}) = 0.044\,52 + 1.036\tilde{T} - 0.889\tilde{T}\tilde{p};$$

low-pressure glass, AP,

$$h(\tilde{p},\tilde{T}) = 0.030\,74 + 0.0215\tilde{p} + 1.457\tilde{T} - 2.26\tilde{T}\tilde{p};$$

high-pressure glass, PF,

$$h(\tilde{p},\tilde{T}) = 0.0347 + 0.0183\tilde{p} + 1.071\tilde{T} - 1.41\tilde{T}\tilde{p};$$

high-pressure glass, AP,

$$h(\tilde{p},\tilde{T}) = 0.023\,91 + 0.0159\tilde{p} + 1.420\tilde{T} - 1.87\tilde{T}\tilde{p}$$

The above expressions are valid between the limits $0.025 \leq \tilde{T} \leq 0.031 + 0.040\tilde{p}$ and $0 \leq \tilde{p} \leq 0.0853$.

For the implementation of the analysis outlined, we note the following relation, defining Young's modulus,

$$F_d - F + p\Delta V = (1/2)(Y + p)\epsilon_1^2 \qquad (6a)$$

with ΔV the deformational volume change, linear in ϵ_1, and F the free energy in the absence of anisotropic strain, as given by eq 7 in the limit $y_d = y$.

The solution of the transcendental equation involved was carried out by using the Brent algorithm[11] for a series of ϵ_1 values up to a maximum value of 2×10^{-3}. A high numerical accuracy is required, since the results are sensitive to changes in y_d, and double precision was employed.

Figures 3–6 display the results for Y, G, and μ as functions of temperature for two pressures and two formation histories. The shear modulus G is given by the relation

$$G = Y/[2(1 + \mu)] \qquad (13)$$

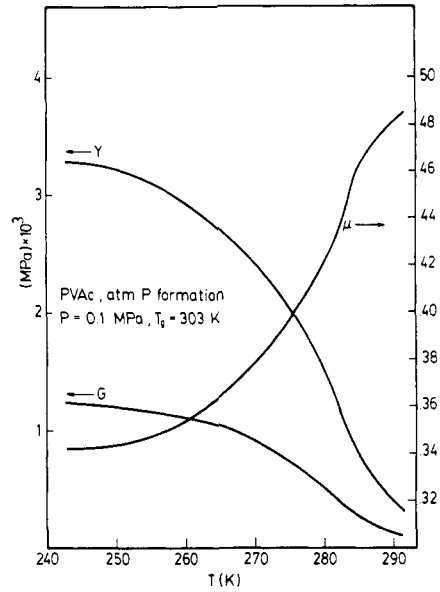

Figure 3. Elastic constants as functions of temperature: PVAc glass formed and held under atmospheric pressure.

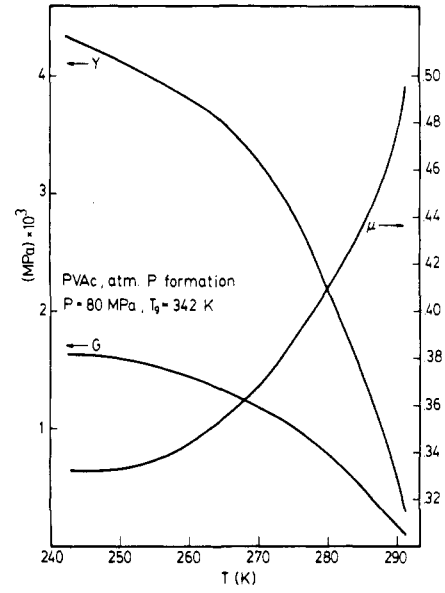

Figure 4. Elastic constants as functions of temperature: PVAc glass formed under atmospheric pressure and held under 80 MPa.

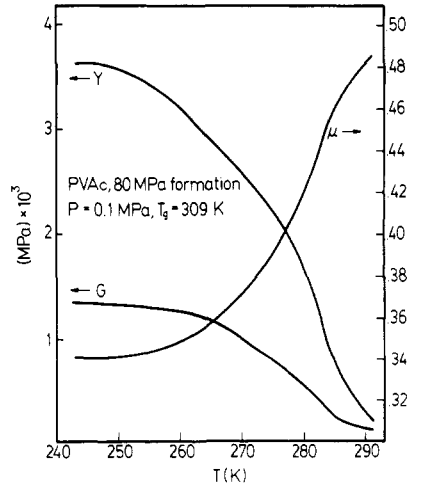

Figure 5. Elastic constants as functions of temperature: PVAc glass formed under 80 MPa and held under atmospheric pressure.

A significant decrease of G and Y with increasing temperature, and much larger than for K, is seen in Figures

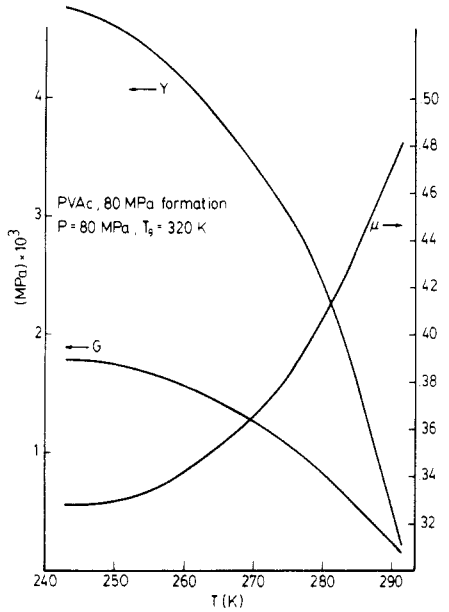

Figure 6. Elastic constants as functions of temperature: PVAc glass formed and held under 80 MPa.

3–6. 4. The maximum increase of G and Y with pressure occurs at the lowest temperature, amounting to about 33 and 40%, respectively, for a pressure increase by 80 MPa. The Poisson ratio, however, remains practically unchanged. Densification by a formation pressure of 80 MPa increases G and Y by maximally 8 and 12%, respectively, with μ decreasing slightly, all at atmospheric pressure; see Figure 5. The densified glass is less pressure sensitive. One notes inflections in the μ-curves in Figures 3 and 5, absent in Figures 4 and 6. This difference arises from the fact that the temperatures in the former are comparatively close to T_g and much farther in the latter. The results shown in these figures are limited by the temperature and pressure range given for h in the undeformed system. An extrapolation of at least the atmospheric pressure results, Figures 3 and 5, to the glass transition temperature is compatible with vanishing values for Y and G and with a value of 0.5 for μ.

The results shown are based on the PF evaluation of y. The analogous computations by means of the AP approximation show practically no differences in respect to Y and maximally only a difference of 5×10^{-3} in μ. A similar situation obtains in the densified glass. These findings suggest that the simple AP procedure should be acceptable in the computation of elastic constants.

Finally we consider as another simplification the use of the compression modulus K(Tait), eq 5, instead of eq 4. At the highest pressure and lowest temperature (−30 °C), this results in an increase of Y by 9% over the PF value. For K the difference is 5%. In the densified system these differences increase to 12 and 8%, respectively. The use of the Tait relation, while providing numerical simplification, is, taken strictly, inconsistent in the present context.

Measurements of static shear or Young's moduli for PVAc do not seem to be available, but one may attempt extrapolations of dynamic results to high frequencies or short times. Knaus and Kenner[12] have determined the shear compliance of PVAc by means of creep measurements. Their sample is stated to have a T_g of 29 °C and, one surmises, contains low molecular weight additives. The glass was prepared by cooling under a pressure of 70 MPa, followed by depressurization. Between −5 and 27.4 °C, it is possible to define a flat portion on a logarithmic time scale. In Figure 7, the extrapolated compliance J is plotted

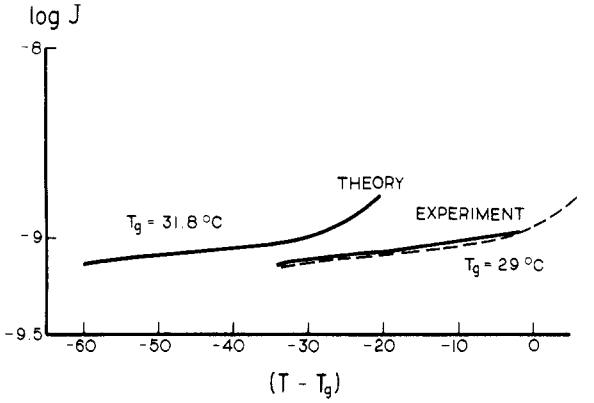

Figure 7. Extrapolated shear compliance of PVAc as a function of temperature distance from T_g; for explanation see text. Solid lines, experiment and theory; scaling pressure and temperature from equation of state of melt. Dashed line, adjustment of scaling temperature.

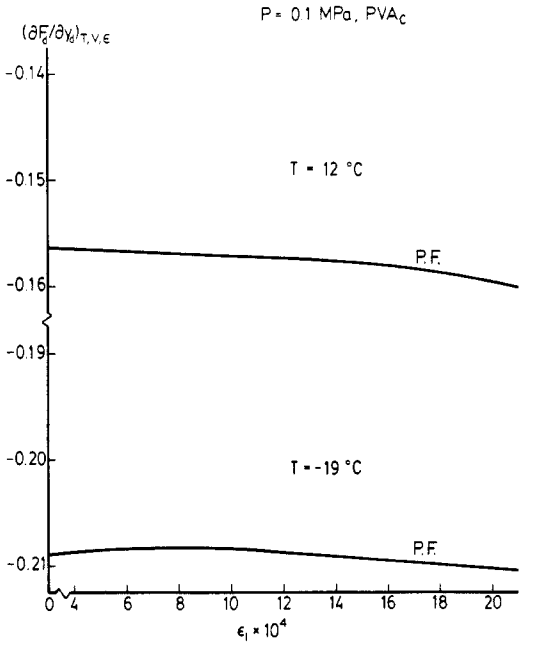

Figure 8. Free energy derivative for PVAc glass formed and held under atmospheric pressure, as a function of strain. PF procedure. For explanation see text.

against the temperature difference $T - T_g$. Three curves are seen: first, the predicted result for the sample of ref 5 and, second, the extrapolation. The theory is formulated in scaled form and here as well as in the previous figures the scaling parameters are derived from the melt. Coincidence between prediction and experiment, the dashed curve, can be accomplished by retaining the previous numerical value of p^*, while changing T* from 9430 to 10380 K. We note that differences of similar magnitudes between different investigators and samples have been seen.[7]

At this point we revert to the previous hypotheses regarding the relation between y, y_d, and free energy derivatives, eq 11 and 12. Figure 8 shows a plot of $(\partial F_d/\partial y_d)_{T,V,\epsilon}$ as a function of strain ϵ_1 for PVAc at atmospheric pressure. One assumption is stipulated strain invariance and the other a zero value, neither of which is satisfied. The following numbers illustrate the sensitivity of the elastic constants to small changes in the free volume fraction $1 - y_d$. At −30 °C, the lowest temperature available, where differences in y_d values are maximized, we have the following values for the low-pressure glass at 0.1 MPa and $\epsilon_1 = 10^{-3}$: correct, 0.0688_4; from volume dependence, eq 11, 0.0702_0; from eq 12a, 0.0725_2; from eq 12b, 0.0712_4.

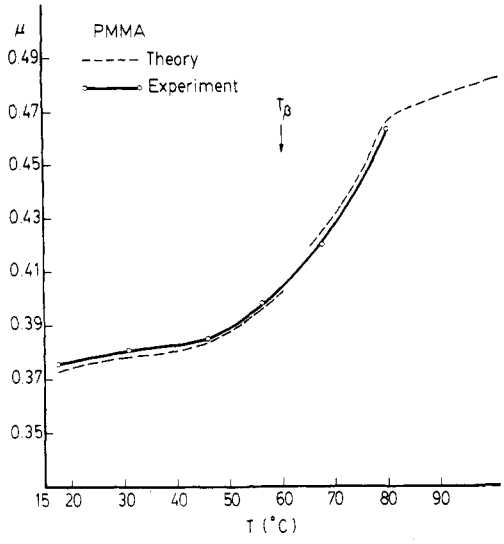

Figure 9. Poisson constant of PMMA as a function of temperature at atmospheric pressure.

Thus considerable accuracy is required in evaluating the deformational free energy. The free volume fraction increases with increasing strain, and at a strain of 0.1% it increases 0.7% over the original value of 0.0683_3. The deformational increase in volume, and hence free volume, is not equivalent to a corresponding change due to an increase in temperature.

B. Poly(methyl methacrylate). We employ the equation of state data of Simha and Wilson,[7,13] at atmospheric pressure with $V^* = 0.8362$ cm^3/g, $T^* = 11\,940$ K. For elevated pressures we have the measurements by Olabisi and Simha.[14] Here the values are $V^* = 0.8350$ cm^3/g, $T^* = 11\,890$ K, and $p^* = 930$ MPa. For our purposes the experimental data were taken from the two theses and y was computed by the AP procedure. The first comparison involves the Poisson ratio, as measured by Yee and Maxwell[15] and shown in Figure 9. The scaling temperature is that given in ref 7. The dilatometric studies[13] locate a β-process at 60 °C at atmospheric pressure and hence a change in the temperature coefficient of y. This is taken into account by the break in the dashed line. The agreement between experiment and prediction is gratifying. The formation history of the glass is not given. But, as noted in the instance of PVAc, it should not play a significant role with respect to μ.

Dynamic data have been published by Maxwell[16] who measured Young's modulus as a function of temperature and frequency under atmospheric pressure. Extrapolation from 1000 Hz yields the results seen in Figure 10. In order to reduce the uncertainties of extrapolation, Y is normalized to the value at 20 °C, and the results are presented again without any adjustment of the scaling temperature. Finally, in Figure 11 the predicted shear and Young's moduli are exhibited. Two sets of curves are seen, namely, for the glasses formed and kept at 0.1 and 200 MPa. Due to the combined effects of formation and actual pressure, significant increments, maximally of 50%, appear for G and Y. Three data points obtained by Fujino[17] have been added. We note the enhanced influence of the β-process at the higher pressure.

4. Discussion

We have arrived at predictions of extensional properties by a generalization of the theory of isotropic compressional properties of polymer glasses. Applications to two polymers under different ambient and formation conditions serve as illustrations. As in preceding contexts, the free

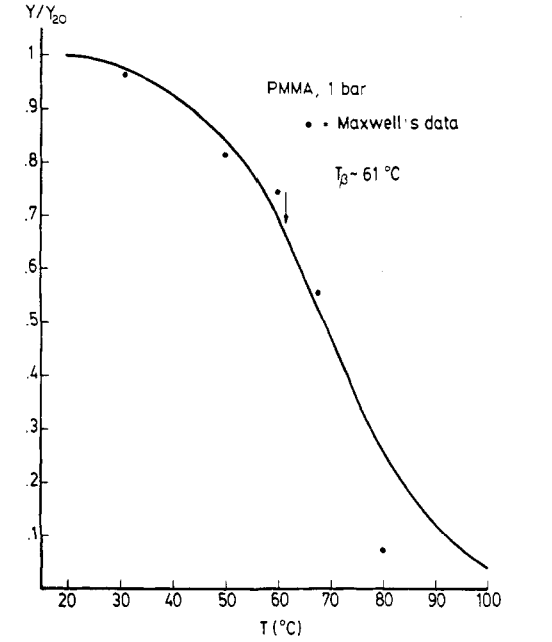

Figure 10. Extrapolated Young's modulus of PMMA as a function of temperature. Points from ref 16. For explanation see text.

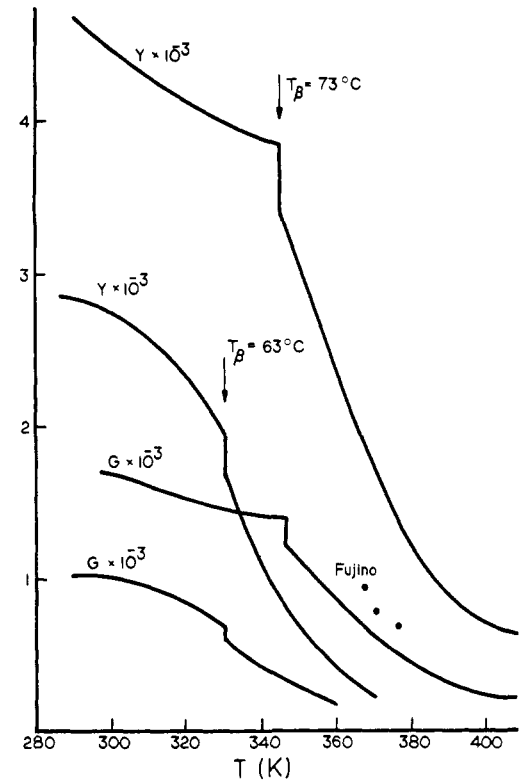

Figure 11. Predicted moduli of PMMA formed and held under 0.1, lower set, and 200 MPa. Points, experimental from ref 17, atmospheric pressure.

volume function continues to play an important role. Equation of state measurements and corresponding theoretical analyses are available for a large number of polymer melts and glasses. Hence elastic moduli can be computed and, in some instances at least, compared with experiment.

Further extensions and uses of the theory may be contemplated. One of these concerns the effect of anisotropic compression stresses. A second topic is a constitutive equation for finite strains ϵ, to be derived by including higher powers of ϵ in the free energy, F_d, or by retaining

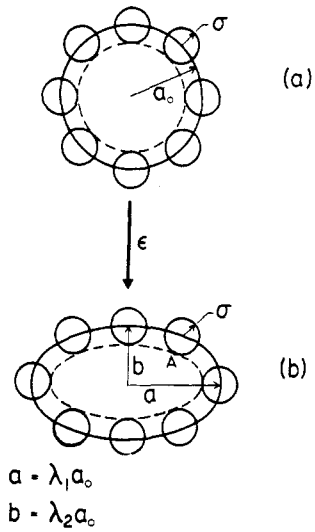

Figure 12. Geometry of $V_{f,s}$, eq A-1, and $V_{f,ds}$, eq A-6.

Table I
PVAc, Atmospheric Pressure Formation

T, °C	a_0	$a_1 \times 10^3$	a_2	a_3
		p = 0.1 MPa		
-30	0.9316_6	-8.128	-503.94	-14929
-9.27	0.9284_6	-4.189	-386.77	-6159
0.15	0.9270_1	-2.428	-358.61	-4756
9.57	0.9255_0	-2.077	-341.19	-4126
18.9	0.9240_9	-1.415	-326.39	-3424
		p = 80 MPa		
-30	0.9348_1	-6.781	-438.48	-9157
-9.27	0.9320_8	-3.384	-360.85	-3723
0.15	0.9307_6	-4.322	-337.11	-4021
11.45	0.9292_5	-3.968	-322.60	-3585
18.9	0.9282_3	-3.477	-316.83	-3947

Table II
PVAc, High-Pressure Formation (80 MPa)

T, °C	a_0	$a_1 \times 10^3$	a_2	a_3
		p = 0.1 MPa		
-30	0.9376_7	11.430	-422.10	-9762
-9.27	0.9353_1	2.981	-334.50	-5196
0.15	0.9342_4	2.999	-318.23	-2359
11.45	0.9329_5	-4.126	-299.03	-4125
18.9	0.9321_0	-1.595	-290.21	-2801
		p = 80 MPa		
-30	0.9392_1	19.770	-400.10	-5323
-9.27	0.9371_2	12.340	-330.68	-3310
0.15	0.9361_7	7.865	-310.80	-3073
11.45	0.9350_2	2.330	-300.88	-2664
18.9	0.9342_6	1.064	-299.44	-1863

the full expression. However, we recall that the chain molecule has been modeled as a collection of segments, each moving in its own cell. Orientation effects were disregarded, but may have to be included in the higher aproximation to F_d. Another comment concerns the kinetics of physical aging. The free volume function has been shown to connect different aging quantities to each other[18,19] and has also served to formulate a kinetics of volume relaxation, following temperature or pressure changes.[20,21] The possibility exists therefore to evaluate aging effects on elastic moduli. Another aspect would be the investigation of volume relaxation, following rapid changes in strain. Finally, we note that the generalization to multiconstituent systems has found a particular application to melt composites. The bulk modulus and thermal expansivity have so far been computed and compared with results of macromechanics.[22,23] A corresponding theory, including extensional moduli, for a glassy matrix would be a further object of investigation.

Table III
PMMA, Atmospheric Pressure Formation

T, °C	a_0	$a_1 \times 10^3$	a_2	a_3
		p = 0.1 MPa		
17.2	0.9369_8	-9.461	-583.18	-26496
31.9	0.9357_7	-5.841	-473.33	-13016
56.8	0.9328_7	-1.611	-379.56	-4678
67.7	0.9311_4	-1.441	-355.47	-4494
80.1	0.9289_6	-2.307	-338.58	-4332
100.9	0.9246_1	-0.975	-311.20	-2789

Table IV
PMMA, High-Pressure (200 MPa) Formation

T, °C	a_0	$a_1 \times 10^3$	a_2	a_3
		p = 200 MPa		
31.9	0.9410_4	-8.680	-407.17	-5863
56.8	0.9405_9	-5.725	-337.85	-3458
67.7	0.9404_9	-5.281	-317.51	-2936
80.1	0.9397_5	-4.138	-304.38	-2963
100.9	0.9375_9	-1.721	-290.04	-2383
124.5	0.9313_0	-0.967	-282.43	-2249

Acknowledgment. This work was supported by the Jet Propulsion Laboratory and funded by the NASA Langley Research Center and by National Science Foundation Grant DMR 84 - 08341.

Appendix

Free Volume and Elastic Constants in a System of Hard Spheres. The solidlike contribution to the free volume in the quasi-lattice arises from the volume available to the reference particle in its own cell when the repulsion volume of the particles at the cell's periphery is taken into account. For the undeformed system with all units smeared over the spherical surface of radius a_0, the free volume is simply a concentric sphere of radius $(a_0 - \sigma)$,[10] where σ is the hard-sphere radius, see Figure 12a, with the following equation:

$$V_{fs}(\epsilon=0) = (4\pi/3)(a_0 - \sigma)^3 \qquad \text{(A-1)}$$

In the deformed system, the free volume equals the volume enclosed by a surface which is defined as the locus of all points a distance σ from the ellipsoidal periphery, see Figure 12b. The following properties suffice to uniquely describe the equation of this surface: (a) The distance between any point $A(x,y,z)$ belonging to the desired locus and point $B(x_s,y_s,z_s)$ on the ellipsoid is constant and equal to σ, i.e.:

$$(x - x_s)^2 + (y - y_s)^2 + (z - z_s)^2 = \sigma^2 \qquad \text{(A-2)}$$

(b) Line AB is normal to the tangent plane at point B on the ellipsoid of axes a and b. Thus

$$(z - z_s)y_s = z_s(y - y_s)$$
$$(z - z_s) = (a^2/b^2)(z_s/x_s)(x - x_s) \qquad \text{(A-3)}$$

taking into account the equation of the ellipsoid:

$$(x_s^2/a^2) + (y_s^2/b^2) + (z_s^2/b^2) = 1$$

The solution of the simultaneous eq A-2 and A-3 yields the locus in question and is most conveniently described by these parametric equations in polar coordinates:

$$x = a \cos\theta[1 - r(\lambda_1 w)]$$
$$y = b \sin\theta \cos\phi[1 - r\lambda_1/(\lambda_2^2 w)]$$
$$z = b \sin\theta \sin\phi[1 - r\lambda_1/(\lambda_2^2 w)] \qquad \text{(A-4)}$$

with $r = \sigma/a_0$ and $w = [1 + (\alpha/\beta)\sin^2\theta]^{1/2}$, where $a = a_0\lambda_1$,

$b = a_0\lambda_2$, $\alpha = (\lambda_1^2 - \lambda_2^2)/\lambda_2^2$, and $\beta = \lambda_2^2$. It is seen that the result represents neither a spherical nor an ellipsoidal surface. For small deformations of course, it approaches a sphere.

The volume of revolution enclosed by this surface is given by the integral

$$V_f = \pi \int f(x)^2 \, dy$$

to be extended over all values of the y-coordinate. Introduction of polar coordinates gives the following result:

$$V_{f,ds} = (4\pi/3)[ab^2(1 - r) + a^2\sigma^2(1 - r)/b^2 - 2a^2\sigma(1 - r) + (\alpha/5\beta)(\sigma b^2 - 4a^3\sigma^2/b^2 + 5a^2\sigma^3/b^2 + 4a^2\sigma - 6a\sigma^2) + (\alpha^2/\beta^2)(-3\sigma b^2/35 + 24\sigma^2a^3/35b^2 - a^2\sigma^3/b^2 - 18a^2\sigma/35 + 32a\sigma^2/35)] \quad (A-5)$$

for arbitrary values of a and b and hence ϵ_1. Since our concern are terms to $\mathcal{O}(\epsilon_1^2)$, expansion of eq A-5 yields

$$V_{f,ds} = (4\pi a_0^3/3)[(1 - r)^3 + (\epsilon_1 - 2\epsilon_2)(1 - r)^2 - \epsilon_1^2(r/5 + 11r^2/5) + \epsilon_2^2(1 - 6r/5 + r^2/5) - 2\epsilon_1\epsilon_2(1 - 4r/5 + r^2)] \quad (A-6)$$

The dimensions of the cell are determined by the 6–12 potential, and hence

$$r = \sigma/a_0 = (r^*/a_0)2^{-1/6} = (v^*/v_0)^{1/3}2^{-1/6} \quad (A-7)$$

where v_0 is the cell volume and r^* the distance corresponding to the minimum of the potential. Equations A-6 and A-7 are then substituted in eq 9.

In a purely repulsive potential of hard spheres the free volume is defined by geometrical considerations solely. Hence the above calculation provides the free energy and the elastic constants of such a system. It is of some interest to pursue this matter for the *cell* model in the absence of attractive forces. This model breaks down for large volumes which would allow the escape of the prisoner from the cell enclosure. At zero strain we have

$$F = -NkT \ln V_f(\epsilon=0) = -NkT \ln \{4\pi(a_0 - \sigma)^3/3\} \quad (A-8)$$

and the equation of state is

$$p = NkT/[V(1 - r)]$$

whence the bulk modulus equals

$$K = NkT(1 - 2r/3)[V(1 - r)^2] \quad (A-9)$$

At small strains, the equivalent of eq A-8 using eq A-6 yields Y as a function of μ. Combined with K (eq A-9) and eq 10, there results a quadratic equation in μ, similar to the earlier derivations,[1,2] viz.,

$$\mu^2(1 - 4r/5 - r^2) + \mu(4.2425 - 7.4710r + 4.8268r^2) - 1.6213 + 3.2355r + 3.6142r^2 \quad (A-10)$$

For close packing of spheres on the cell periphery, we have $r = 0.258$ and with a coordination number of 12, $\mu = 0.19$. At $r = 0.13$, escape from the cage is possible, and $\mu = 0.31$. The inclusion of an attractive potential at $T = 0$ raises the minimum value to 0.25.[1]

Data for the strain dependence of the free volume function $1 - y_d$, $y_d = \sum_{i=0}^{3} a_i\epsilon_1^i$ are given in Tables I–IV.

Registry No. PVAc, 9003-20-7; PMMA, 9011-14-7.

References and Notes

(1) Peng, S. T. J.; Landel, R. F.; Moacanin, J.; Simha, R.; Papazoglou, E. *J. Rheol.* **1987**, *31*, 125.
(2) Papazoglou, E.; Simha, R. *J. Rheol.* **1987**, *31*, 135.
(3) Simha, R.; Roe, J. M.; Nanda, V. S. *J. Appl. Phys.* **1972**, *43*, 4312.
(4) Midha, Y. R.; Nanda, V. S. *Macromolecules* **1977**, *10*, 1031.
(5) For example: McKinney, J. E.; Simha, R. *Macromolecules* **1974**, *7*, 894; **1976**, *9*, 430.
(6) Papazoglou, E.; Simha, R. *Bull. Am. Phys. Soc.* **1987**, *32*, 424.
(7) Simha, R.; Wilson, P. S. *Macromolecules* **1973**, *6*, 908.
(8) Weiner, J. H. *Statistical Mechanics of Elasticity*; Wiley: New York, 1983.
(9) Simha, R.; Somcynsky, T. *Macromolecules* **1969**, *2*, 342.
(10) Prigogine, I. *The Molecular Theory of Solutions*; North Holland: Amsterdam, 1957.
(11) Brent, R. P. *Comput. J.* **1971**, *14*, 422.
(12) Knaus, W. G.; Kenner, V. H. *J. Appl. Phys.* **1980**, *51*, 5131.
(13) Wilson, P. S.; Simha, R. *Macromolecules* **1973**, *6*, 902. Wilson, P. S. Ph.D. Thesis, Case Western Reserve University, 1973.
(14) Olabisi, O.; Simha, R. *Macromolecules* **1975**, *8*, 206, 211. Olabisi, O. Ph.D. Thesis, Case Western Reserve University, 1975.
(15) Yee, A. F.; Maxwell, M. A., cited in Hong, et al. (Hong, S. D.; Chung, S. Y.; Fedors, R. F.; Moacanin, J. *J. Polym. Sci., Polym. Phys. Ed.* **1983**, *21*, 1647).
(16) Maxwell, B. *J. Polym. Sci.* **1956**, *20*, 551.
(17) Fujino, K.; Senshu, K.; Kawai, H. *J. Colloid Sci.* **1961**, *16*, 262.
(18) Curro, J. G.; Lagasse, R. R.; Simha, R. *J. Appl. Phys.* **1981**, *52*, 5892.
(19) Lagasse, R. R.; Curro, J. G. *Macromolecules* **1982**, *15*, 1559.
(20) Curro, J. G.; Lagasse, R. R.; Simha, R. *Macromolecules* **1982**, *15*, 1621.
(21) Robertson, R. E.; Simha, R.; Curro, J. G. *Macromolecules* **1984**, *17*, 911; **1985**, *18*, 2239.
(22) Simha, R.; Jain, R. K.; Jain, S. C. *Polym. Compos.* **1984**, *5*, 3.
(23) Simha, R.; Jain, R. K.; Maurer, F. H. J. *Rheol. Acta* **1986**, *25*, 161.